

Effects of Post Deposition Treatments on Vacuum Evaporated $CdTe$ Thin Films and $CdS/CdTe$ Heterojunction Devices

Habibe BAYHAN, Çiğdem ERÇELEBİ
Middle East Technical University
Department of Physics, 06531 Ankara - TURKEY

Received 02.04.1997

Abstract

$CdTe$, CdS thin films and $n - CdS/p - CdTe$ heterostructures have been prepared by conventional vacuum evaporation technique. Some post deposition treatments to optimize the device efficiency have been analyzed and the effects of the individual process steps on the material and device properties were investigated. Annealing in air with and without $CdCl_2$ -treatment decreased the $CdTe$ resistivity. The $CdCl_2$ -dip followed by annealing in air at $300^\circ C$ for 5 min improved the grain size and polycrystalline nature of $CdTe$ thin films. Solar efficiency improvements were achieved when heterojunctions were prepared on successively treated (i.e. etched, air annealed, $CdCl_2$ -processed) $CdTe$ surfaces. Etching of the $CdTe$ surface with potassium dichromate solution prior to metal contact deposition lead to the formation of low-resistance Au contacts and increase in open circuit voltage and fill factor values.

1. Introduction

Cadmium telluride and cadmium sulfide thin films have been extensively studied for their applications in heterojunction solar cells. Several deposition methods, including the vacuum evaporation technique have been successively used to prepare $CdS/CdTe$ heterojunctions with photovoltaic conversion efficiencies in excess of 10 % [1-3 and the references therein]. The optimized properties of $CdTe$ thin film and the $CdS/CdTe$ interface with post deposition treatments, are believed to play an important role in solar cell operation. These treatments commonly involve high temperature annealing in oxygen containing atmosphere at $400^\circ C$ or higher. It has been reported that after the heat treatment in air at $550^\circ C$, vacuum evaporated intrinsic $CdTe$ films become p -type [4] and the type conversion n - to p -type of $CdTe$ layer have been developed for the electrodeposited films with the heat treatment at around $400^\circ C$ in oxygen containing

ambient [5]. The other basic ingredient $CdCl_2$ is either introduced during or after the film deposition process [6-8]. Although the actual physical processes taking place in these beneficial procedures are still a matter of discussion, the quality of $CdTe$ film is always improved. Grain growth [1, 6], reduction of interface recombination and generation of recombination centers in the space charge region [9] have been observed. The formation of a $CdTe_{1-x}S_x$ interlayer with a decrease in the band gap was also seen in the physical vapor deposited [8] and screen printed [10] $CdS/CdTe$ cells.

In this paper we present the studies on the $CdS, CdTe$ thin films and $Au - CdTe/CdS-TO$ heterojunctions prepared by conventional vacuum evaporation technique in view of the post deposition processing steps applied to $CdTe$ layer prior to device completion. Different post processing steps and the effects on the material properties of the undoped-doped and antimony doped $CdTe$ films; the device properties of the heterojunctions are discussed.

2. Experimental

$CdTe$ and CdS thin films were deposited by thermal evaporation in oil pumped vacuum systems operating at about 10^{-6} Torr. Source and substrate temperatures were kept at about $800^\circ C$ and $200^\circ C$ for CdS ; $650^\circ C$ and $200^\circ C$ for $CdTe$ films, respectively. The films were deposited onto cleaned glass slides in a six-arm bridge and Maltese-cross shapes for resistivity measurements. Contacts to $p - CdTe$ and $n - CdS$ were made by subsequent evaporation of 300-400 Å of gold and indium electrodes followed by annealing at $200^\circ C$ in nitrogen atmosphere for 5 min, respectively. Heterojunction solar cells were prepared by the successive deposition of $CdS, CdTe$ layers and circular Au electrodes onto tin oxide coated glass substrates. The sheet resistance of the TO was approximately 10 ohms/square.

To investigate the effects of each post deposition treatments and the chemical etching on the properties of the vacuum evaporated $CdTe$ films and $CdS/CdTe$ heterojunctions, the surfaces of $CdTe$ layers were subjected to different processing steps. The samples were labelled as follows;

- G1: as-grown;
- G2: chemical etching and DI-water rinse;
- G3: annealing in air at different temperatures;
- G4: annealing in air at different temperatures, chemical etching and DI-water rise;
- G5: dipping in $CdCl_2 : CH_3OH$ (1/100) solution for 2-5 sec, drying without rinsing and annealing in air at different temperatures;
- G6: dipping in $CdCl_2 : CH_3OH$ (1/100) solution for 2-5 sec, drying without rinsing, annealing in air at different temperatures, chemical etching and DI-water rinse.

The chemical etchant, annealing temperature and time are $K_2Cr_2O_7 : H_2SO_4 : H_2O$ (7 gm: 3 gm: 50 ml); 300 – 400°C and 5 to 10 min, respectively.

The films were characterized at each processing step by X-ray diffractometer with cobalt K_α radiation; Reflection of High Energetic Electron Diffraction, RHEED; Scanning Electron microscopy, SEM. A Keithley 220 programmable constant current source and Keithley's 616 digital electrometer were used for the electrical characterization of the films and heterostructures. The resistivities of $CdTe$ films in parallel direction to the substrate were measured with the help of a Keithley's 8002A high resistance test fixture. The photovoltaic performances of the heterostructures were measured under a simulated solar source of 80 mW cm^{-2} through the CdS/TO side of the junction.

3. Results and Discussion

3.1. Properties of $CdTe$ and CdS Thin Films

In general, two problems were encountered with $CdTe$ films for device applications; stable and low resistance ohmic contact formation and controlling of p -type conductivity. A number of different attempts have been reported for achieving good contacts to high resistivity $p - CdTe$ films prepared with various techniques [11-13]. The commonly used chemicals were KOH and Bromine-in-methanol which dissolve $CdTe$ rapidly leaving behind low resistive p -regions. In the present study, gold and $K_2Cr_2O_7 + H_2SO_4 + H_2O$ solution have been used as for the contact material and the chemical etchant, respectively, and the contacts were found to be quite stable after heating them at 200°C for 5 min in nitrogen atmosphere. Almost linear and bias independent nature of log I-log V characteristics of both Hall-bar and $Au - CdTe - Au$ sandwich structures indicated the ohmic nature of gold contacts. A relatively great decrease in the specific contact resistivity values from about $10^5 \Omega cm^2$ to a few Ωcm^2 was observed after annealing of the Au contacts on chemically etched $CdTe$ surface. Since dichromate etch produces excess Te on the $CdTe$ film surface, it is likely that consumption of excess Te by Au contact leaves behind a rather stoichiometric surface [14] deteriorating the tunneling junction necessary for good ohmic behavior.

The resistivity values measured for a representative group of $CdTe$ films annealed at 300 – 400°C for 5-10 min are tabulated in Table 1. All as-grown films with no intentional doping have high resistivity and attempts to dope $CdTe$ by antimony to obtain more p -type conducting films with lower resistivity resulted a decrease in the resistivity by 1-2 orders of magnitude.

The decrease in the resistivity of $CdTe$ films grown by CSS has been reported when such films doped with antimony depending on the dopant concentration [15], but the attempts to dope the HWVE $CdTe$ films with antimony during deposition by co-evaporation have been reported to be unsuccessful [16]. Control of Sb doping from the vapor phase is more difficult, because antimony forms Sb_2 and is not incorporated at

low antimony pressure; at high antimony pressure, metallic precipitation form and the conductivity increase discontinuously [17]. In the past several years, to enhance doping efficiency and materials quality, hybrid techniques are being successfully introduced, such as ion-Assisted Doping and Growth (IAD and IAG), and Photon-Assisted Doping and Growth (PAD and PAG) [18]. Oxygen is known to change the effective carrier concentration and enhance the p -type conductivity of $CdTe$ films when such films are annealed in oxygen containing atmosphere at high temperatures i.e., $400 - 500^\circ C$ for at least 30 min [14, 19, 20]. Birkmire et.al. [4] found that vacuum evaporated as-deposited $CdTe$ film was of intrinsic type with resistivity higher than 10^7 ohm cm, but after heat treatment in air at $550^\circ C$ for 4 min, the films become p -type with resistivity of 10^4 ohm cm. Analyses showed that for annealing temperatures below than $400^\circ C$, no change occurred in resistivity of $CdTe$ films in 15 min time interval. However, in this work, a systematic decrease in resistivity was observed with the increase of annealing temperature and time interval (Table 1). Annealing at higher temperatures ($> 400^\circ C$) and/or for longer durations (> 10 min) were found to degrade film properties by the creation of shorting paths through the pinholes created. The lowest resistivities were obtained when $CdCl_2$ -dip was included into the processing scheme. Even though the resistivity of the $CdTe$ films consistently decreases as the annealing temperature and time increases; the best device parameters are attained for the heterostructures annealed at $300^\circ C$ for 5 min, as discussed in sec. 3.2. Thus the results of the structural and morphological studies are presented for the films attained at these conditions.

Table 1. Measured resistivity values of the undoped and antimony doped $CdTe$ films.

	Resistivity $\rho(\Omega\ cm)$	
	Undoped	Sb doped
As-grown	$\geq 10^{10}$	2.5×10^8
Annealed at $300^\circ C$ for		
-5 min.	5.0×10^8	4.8×10^7
-10 min.	2.3×10^8	2.8×10^7
Annealed at $400^\circ C$ for 10 min	1.8×10^8	1.5×10^7
$CdCl_2$ -dipped + annealed at $300^\circ C$ for		
-5 min.	9.2×10^7	4.6×10^6
-10 min.	5.2×10^7	2.8×10^6
$CdCl_2$ -dipped + annealed at $400^\circ C$ for 10 min.		
10 min.	4.8×10^7	1.5×10^6
$CdCl_2$ -dipped + annealed + etched at $300^\circ C$ for		
-5 min.	3.6×10^7	2.7×10^6
-10 min.	2.6×10^7	2.1×10^6
$CdCl_2$ -dipped + annealed at $400^\circ C$ for 10 min. + etched	2.0×10^7	9.7×10^5

All the $CdTe$ films grown onto glass substrates were polycrystalline in nature and had cubic zincblende type structure. The X-ray diffraction spectrum of as-deposited films displayed a strong peak associated with corresponding (111) planes of cubic zincblende $CdTe$. However, some other peaks have developed after the application of each post deposition processing, as shown in Figure 1. Upon annealing, principal diffraction peaks corresponding to (220), (311), (400) and (331) planes of cubic $CdTe$ appeared. There were also some unidentified peaks which may have been due to TeO_2 . The intensity of the (220) planes decreased considerably after $CdCl_2$ -processing. The additional diffraction peaks observed were possibly due to $CdCl_2$, $TeCl_2$ and Te_2 . Additional peaks related to Sb were observed when the doped films were considered. Similar results have also been obtained from the analysis of RHEED patterns of the samples. Estimated average grain sizes ϵ , obtained from the diffraction peaks associated with the (111) planes of cubic $CdTe$ (i.e. line broadening at fullwidth half maximum (FWHM), [21]), were found to increase from 75-85 nm for the as-grown and air annealed, respectively, to about 100 nm for the $CdCl_2$ -processed films.

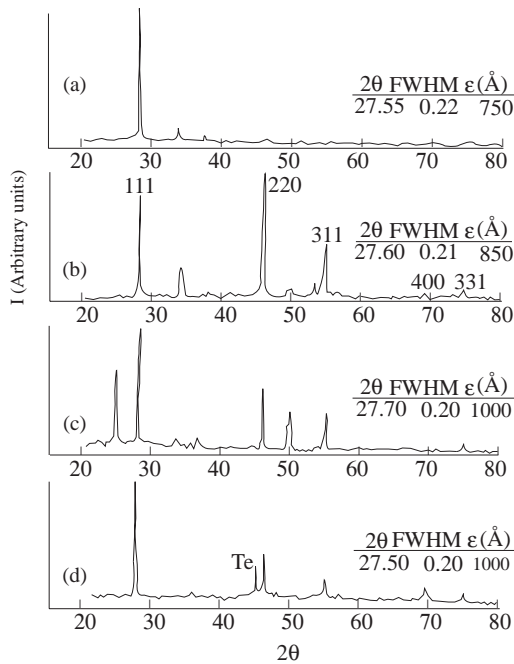


Figure 1. Representative X-ray diffraction spectra for the (a) as-grown, (b) air annealed, (c) $CdCl_2$ -dipped + air annealed and (d) $CdCl_2$ -dipped + annealed + etched $CdTe$ thin films.

The evaporated CdS films were found to have polycrystalline nature and grown in the hexagonal wurtzite structure with strongly preferred orientation along the {0002}

plane parallel to substrate as revealed from X-ray diffraction, SEM and RHEED studies. The resistivities of the samples were controlled by indium doping and found to be in between 0.3 to 7 $\Omega\text{ cm}$.

3.2. Device Characterization

The photovoltaic performances of the samples were researched on the basis of following device groups prepared as explained in Sec. 2;

- G1: $Au - CdTe/CdS - TO$ (as-grown devices),
- G2: Au -(etched) $CdTe/CdS - TO$,
- G3: Au -(annealed) $CdTe/CdS - TO$,
- G4: Au -(etched+annealed) $CdTe/CdS - TO$,
- G5: Au -(annealed+ $CdCl_2$ -dipped) $CdTe/CdS - TO$,
- G6: Au -(etched+annealed+ $CdCl_2$ -dipped) $CdTe/CdS - TO$.

It was found that, independent of the group considered, annealing the samples after Au contact evaporation at about $200^\circ C$ for 5 min in N_2 atmosphere increases the open circuit voltage and the short circuit current due to the improvement of the ohmic behavior of the Au contact. The illuminated I-V characteristics illustrated in Figure 2 (a) and (b) are for the typical heterojunction devices with undoped and Sb doped $CdTe$ after the contact annealing, respectively. All the samples considered had almost an equal active cell area of about 0.03 cm^2 .

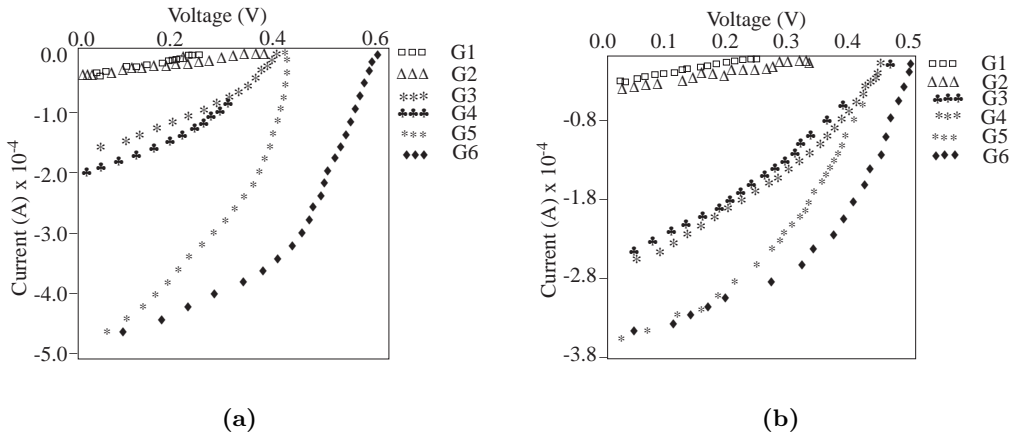


Figure 2 Illuminated I-V characteristics of the typical devices of various groups with (a) undoped, (b) Sb doped $CdTe$ layer.

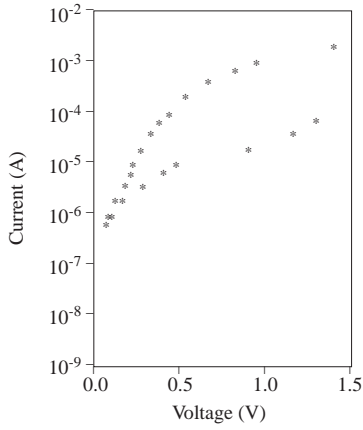
Table 2. Photovoltaic parameters of typical $Au - CdTe/CdS - TO$ heterojunction solar cells produced with (a) undoped and (b) Sb doped $CdTe$ layers.

	(a)				(b)			
	V_{oc} (V)	I_{sc} (mA/cm^2)	FF	η %	V_{oc} (V)	I_{sc} (mA/cm^2)	FF	η %
G1	0.26	1.30	0.28	0.12	0.25	1.30	0.28	0.10
G2	0.38	1.30	0.28	0.20	0.33	1.30	0.28	0.15
G3	0.41	5.70	0.35	1.00	0.48	8.35	0.33	1.60
G4	0.40	6.70	0.36	1.20	0.45	8.70	0.36	1.80
G5	0.41	16.00	0.40	3.30	0.46	12.00	0.40	2.80
G6	0.58	16.00	0.50	5.80	0.50	11.70	0.47	3.50

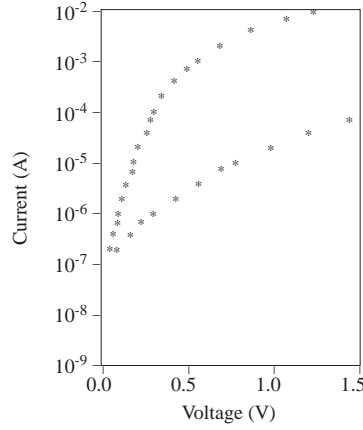
Analysis of the illuminated I-V characteristics of the samples from each group (G1 to G6) demonstrated the best conditions for the post deposition processing steps giving rise to improved cell performances in a significant manner (Table 2). The performance characteristics of the as-grown samples (G1) were very poor with conversion efficiencies of about 0.1-0.12 %. This was probably due to the high resistive $CdTe$ layer, even doped with antimony, some leakage current through pin-holes in the $CdTe$ layer, defects at the $CdS/CdTe$ interface and non-optimum back contact formation. The better photovoltaic parameters obtained after chemical etching (G2, G4 and G6) was attributed to the Te rich surface leading to tunneling type contact formation as well as the decrease in recombination losses at the contact-film interface and decrease of the series resistance. A substantial increase in solar efficiency was observed when annealing in air was introduced both before and after the $CdCl_2$ -dipping (G3-G6) and the best results were attained at $300^\circ C$ for 5 min. These were probably as a result of a better $p - n$ junction formation with a fewer pin-hole and lower interface state densities, respectively. Even though the temperature and the time used in this work seem to be low to observe an enhancement of p -type character of the layer, the decrease in the resistivity when compared the results of the relevant studies, the specifics of the heating process have been reported to vary with the deposition technique used as well as the specifics of the post-deposition heat treatments [22]. The most important improvement in the device efficiency was obtained when dipping into $CdCl_2$ solution was followed by annealing at $300^\circ C$ for 5 min. and chemical etching (G6). The introduction of the $CdCl_2$ processing affects not only the $CdTe$ film properties but also the $CdS/CdTe$ film interface leading to the remarkable increase in the device efficiency. The observed grain growth and decrease in intergrain pore size are expected after $CdCl_2$ -dipping to reduce the bulk and interface state density. Also, $CdCl_2$ is known to cause intermixing of CdS and $CdTe$ at the interface [8, 10] which presumably causes the shift of the heterojunction from the metallurgical interface into $CdTe$, improving the electrical properties of the $CdS/CdTe$ junction. The highest efficiencies obtained at this stage are about 6 % and 3.5 % for devices with undoped and Sb doped $CdTe$ layers, respectively, but are low compared

to the reported values for the vacuum deposited cells [4, 8]. However, for the efficiency calculations, contact optimization studies were not carried out and heterostructures had no antireflection coatings. The photovoltaic characteristics of undoped samples were found to be effected more with the applied processing steps, especially with $CdCl_2$ -dipping. Although, the physics behind it is not clear, which will be investigated in future, the role of Sb doping might be incorporated with the applied processing steps through creation of some performance limiting defect levels.

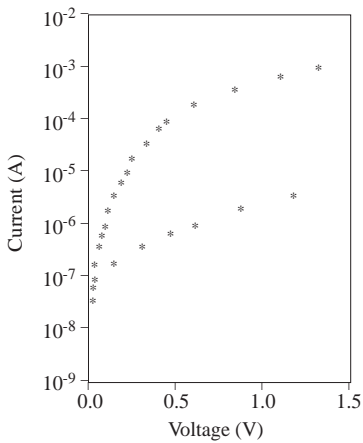
The room temperature dark forward and reverse log I vs V plots of the same group of undoped samples are illustrated in Figure 3. The forward current-voltage characteristics can be expressed by the standard diode equation,



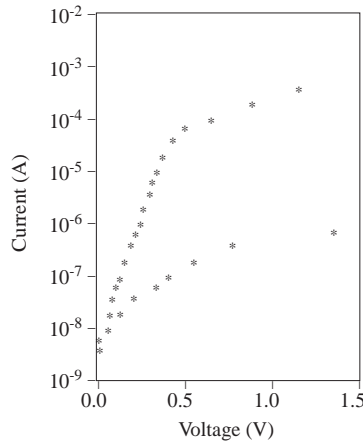
(a)



(b)



(c)



(d)

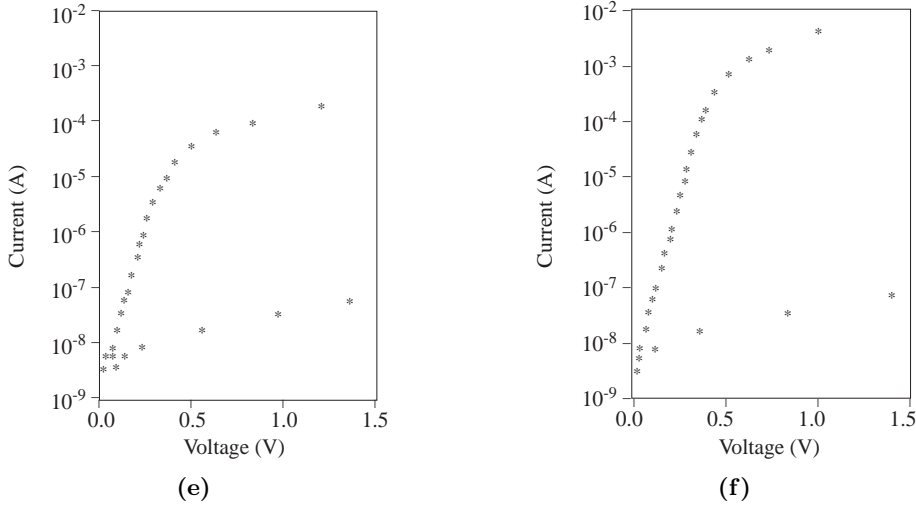


Figure 3. Room temperature dark I-V characteristics of typical devices from groups (a) G1, (b) G2, (c) G3, (d) G4, (e) G5 and (f) G6.

$$I = I_0 \exp(qV/nkT),$$

where n is the diode ideality factor, I_0 is the reverse saturation current; and k, q have their usual meanings. The general improvement in the conductivity as a result of chemical etching, annealing and $CdCl_2$ -dipping of the $CdTe$ films is evident through the decrease in n, I_0 and increase in the rectification factor (Table 3). The chemical etching of the $CdTe$ surface with $K_2Cr_2O_7 + H_2SO_4 + H_2O$ solution prior to Au contact evaporation is found to be essential for the improvement of the diode behavior. The deviations of the I-V plots from the exponential behavior at high biases are attributed to the series resistance effects which become less dominant when the etching of the $CdTe$ surface was employed. This might result from the decrease in the contact and/or bulk resistivity values after chemical etching. The best diode parameters were reached when the $CdTe$ surface was dipped in $CdCl_2$, annealed in air and then chemically etched. Almost similar results have been obtained from the I-V plots of Sb doped devices.

4. Conclusions

The individual effects of different post deposition treatments, such as air annealing, $CdCl_2$ -dipping applied to vacuum evaporated $CdTe$, on the material and $Au - CdTe/CdS - TO$ heterojunction device properties have been investigated. $CdTe$ films were all p -type, polycrystalline in nature and had cubic zincblende structure under given deposition conditions. The undoped films were highly resistive, and doping the films with antimony decreases the resistivity of the films several orders of magnitude.

Table 3. The diode ideality factor n , reverse saturation current I_0 and rectification factor R , values for the typical devices of various groups with undoped $CdTe$ layer.

Sample Group	n	$I_0(A)$	R (at IV)
G1	2.80	4.0×10^{-7}	80
G2	2.20	1.5×10^{-7}	200
G3	2.50	1.0×10^{-7}	260
G4	1.76	9.0×10^{-9}	600
G5	1.30	6.0×10^{-9}	4.6×10^3
G6	1.33	3.0×10^{-9}	4.0×10^4

The resistivity of both doped and undoped films decreased systematically when films were subjected to heat treatment at $300 - 400^\circ C$ for 5-10 min and to $CdCl_2$ treatment. But any further increase in temperature and time created some shorting paths through the pin holes. An increase in the estimated grain size values was observed when $CdCl_2$ treatment was performed but almost no grain growth observed only with annealing. At this stage we conclude that $CdCl_2$ behaves as a fluxing agent for recrystallization, which improves the grain size and polycrystalline nature of the $CdTe$ film. Etching the $CdTe$ surface prior to Au deposition with $K_2Cr_2O_7 + H_2SO_4 + H_2O$ solution and post annealing of the structure at $200^\circ C$ for 5 min was found to be necessary for the improvement of the device efficiency. Even though an improvement both in diode and photovoltaic performances were observed for $Au - CdTe/CdS - TO$ heterojunctions with Sb doped and undoped $CdTe$ layer, best results are attained when the $CdCl_2$ dipping is followed by annealing in air at $300^\circ C$ for 5 min with the undoped $CdTe$ film. The aim of this study was to investigate in detail the influence of the post-deposition treatments on the material and device properties of the vacuum deposited thin film $CdS/CdTe$ heterostructures which lead to better control of the growth and sample preparation conditions to improve the $CdTe$ film and device quality.

Acknowledgements

The authors are grateful to the II-VI Group of Physics Department at University of Durham for the collaboration in performing the structural studies and are also grateful to the British Council for the financial support.

References

- [1] B.M. Bařol, Doęa, Tr. J. Phys., **16** (1992) 107.
- [2] D. Bonnet, Int. J. Sol. Energy, **12** (1992) 1.
- [3] T.L. Chu and S.S. Chu, Solid-Stat Elec., **38** (1995) 533.

BAYHAN, ERÇELEBİ

- [4] R.W. Birkmire, B.E. McCandless and W.N. Shafarman, *Sol. Cells*, **23** (1988) 109.
- [5] B.M. Başol, *J. Appl. Phys.*, **55** (1984) 601.
- [6] B.M. Başol, *Int. J. Sol. Energy*, **12** (1992) 25.
- [7] S.A. Ringel, A.W. Smith, M.H. MacDougal and A. Rohatgi, *J. Appl. Phys.*, **70** (1991) 881.
- [8] R.W. Birkmire, B.E. McCandless and S.S. Hegedus, *Int. J. Sol. Energy*, **12** (1992) 145.
- [9] A. Rohatgi, *Int. J. Sol. Energy*, **12** (1992) 37.
- [10] Y.S. Seol and H.B. Im., 9th European Photovoltaic Conference, Freiburg (1989).
- [11] E. Janik and R. Triboulet, *J. Phys. D. Appl. Phys.*, **16** (1983) 2333.
- [12] J. Ponpon, *Solid State Electron*, **28** (1985) 689.
- [13] B. Ghus, S. Porakayastha, P.K. Datta, R.W. Miles and M.J. Carter, *R. Hill, Semicond. Sci. Technol.*, **10** (1995) 71.
- [14] B.M. Başol, S.S. Ou and O.M. Stafsudd, *J. Appl. Phys.*, **58** (1985) 3809.
- [15] T.L. Chu and S.S. Chu, *Int. J. Sol. Energy*, **12** (1992) 121.
- [16] R.H. Bube, *Solar Cells*, **23** (1988) 1.
- [17] A.L. Fahrenbruch, *Solar Cells*, **21** (1987) 399.
- [18] A.L. Fahrenbruch, R.H. Bube, D. Kim and A. Lopez-Otero, *Int. J. Sol. Energy*, **12** (1992) 197.
- [19] Y.S. Tyan, F. Vazan and T.S. Berge, in: *Proc. 17th IEEE Photov. Spec. Conf. 1984* (IEEE, New York, 1984) p.840.
- [20] S. Ikegami and A. Nakano, *Int. J. Sol. Energy*, **12** (1992) 53.
- [21] B.D. Cullity in "Elements of X-Ray Diffraction", (Addison Wesley Press, 1956).
- [22] F.A. Abou-Elfotough, H.R. Moutinho, F.S. Hasoon, R.K. Ahrenkiel, D. Levi and L.L. Kazmerski, in: *Proc. 23rd IEEE Photov. Spec. Conf. Louisville* (1993).

CONTENTS

<i>The Submillimeter-Wave Rotational Spectrum of Isopropyl Alcohol (trans-form)</i>	363
C. QAJAR, S. MUSAEV	
<i>Shallow Donors in a Quantum Well Wire: Electric Field and Geometrical Effects</i>	369
M. ULAŞ, H. AKBAS, M. TOMAK	
<i>The Effect of Exposure Time to Clean Room Air on Characteristic Parameters of Au/Epilayer n – Si Schottky Diodes.....</i>	377
M. SAĞLAM, Ç. NUHOĞLU, E. AYYILDIZ, A. TÜRÜT, H. A. ÇETİNKARA	
<i>Resonans Reflectionless Absorption of Electromagnetic Waves In Solutions ...</i>	389
E. SALAEV, E. GASIMOV, S. AZIZOV, J. QAJAR	
<i>$\tau \rightarrow \rho\nu$ Decay and Leptonic Decay Constants of Vector Mesons.....</i>	395
Kh. ABLAKULOV, B. N. KURANOV, T. Z. NASYROV	
<i>Resonance Production of New Resonances at ep and γp Colliders</i>	401
A. ÇELİKEL, M. KANTAR	
<i>Determination of Temperature Dependent Frequency Factor Constant from TL Glow Curves</i>	415
A. N. YAZICI	
<i>Quaternionic Roots of E_8 Related Coxeter Graphs and Quasicrystals</i>	421
M. KOCA, N. Ö. KOCA, R. KOÇ	
<i>Effect of Sintering Time On Sb Added BiPbSrCaCuO Superconducting Ceramics</i>	437
K. KOCABAŞ	
<i>Effects of Post Deposition Treatments on Vacuum Evaporated CdTe Thin Films and CdS/CdTe Heterojunction Devices</i>	441
H. BAYHAN, Ç. ERÇELEBİ	